Identity Recognition of Multi-Haptic Pressure Feature based on Sparse Representation

Yan Zhang[1]
[1]Key Laboratory of Intelligent Computing and Signal Processing of Ministry of Education, School of Physics and Materials Science, Anhui University, Hefei, Anhui 230039, China
zhangyaner2005@163.com

Dong Liang[2*]
[2]School of Electronics and Information Engineering, Anhui University, Hefei, Anhui 230039, China
dliang@ahu.edu.cn

Ming Zhu[1,2]
[1]Key Laboratory of Intelligent Computing and Signal Processing of Ministry of Education, [2]School of Electronics and Information Engineering, Anhui University, Hefei, Anhui 230039, China
zhu_m@163.com

Wenxia Bao[1,2]
[1]Key Laboratory of Intelligent Computing and Signal Processing of Ministry of Education, [2]School of Electronics and Information Engineering, Anhui University, Hefei, Anhui 230039, China
bwxia@ahu.edu.cn

***Abstract*: Herein, a new identity recognition method of multi-haptic pressure feature based on sparse representation was investigated. According to the common dynamic features, the regional feature and the ratio of length vs. width of external bounding rectangle (extracted by using the least area method) were extracted. The subset of dynamic feature was optimized by correlation criterion, the sparse representation of haptic pressure was obtained according to the sparse basis (i.e., wavelet basis), and the sparse feature vector was calculated by the Topelitz measurement matrix. After that, the haptic pressure feature set was created by combining dynamic feature subset and sparse feature subset linearly. Furthermore, Support Vector Machine (SVM) classifier identified more than two objects following the one to many rule and output the identification result according to the rule of majority voting, and the stability of features is studied by calculating the intraclass correlation coefficient (ICC) and coefficient of variation (C.V). Overall, the improved acuracy of identity recognition demonstrating the effectiveness and stability of the multi-haptic pressure feature.**

***Keywords:* dynamic feature, sparse representation, optimization, correlation criterion, recognition**

1. INTRODUCTION

Biometric features, such as fingerprint and facial characteristic, have attracted growing interests and have been widely used for inherent physiology. As a branch of biometrics, haptic pressure has been used for motion measurement, medical rehabilitation, and disease diagnosis [1,2]. Biometrics research efforts have indicated that the information of haptic pressure is unique and repetitive, demonstrating the effectiveness and stability for identity recognition and footprint tracking[3,4]. In the past several years, simple haptic pressure dynamic features have been used to detect diabetic foot; it has also been studied for security systems in special occasions/locations, such as airports and customs [5]. The platform system, developed by Intelligent Machines Institute of the Chinese Academy of Sciences, has been typically adopted to collect the common haptic pressure features such as the maximum pressure, contact area, mean pressure, pressure center, and the geometric center line [6,7].

In this study, according to the characteristics of haptic pressure, a new identity recognition method of multi-haptic pressure feature based on sparse representation (MHPF-RS) was investigated. During the study, the whole foot was divided into five regions. Based on the common dynamic features the regional features were extracted, and the ratio of length vs. width of external bounding rectangle was acquired by using the least area method. Subset of dynamic features was optimized by correlation criterion. The sparse representation of haptic pressure was then obtained according to the sparse basis (i.e., wavelet basis). Thereafter, sparse feature vector was calculated by the Topelitz measurement matrix, and the haptic pressure feature set was obtained by combining optimized dynamic feature subset and sparse feature subset. Furthermore, Support Vector Machine (SVM) classifier identified more than two objects following the one to many rule and output the identification result according to the rule of majority voting. The stability of identity recognition was further studied by calculating the intraclass correlation coefficient (ICC) and coefficient of variation (C.V). The results indicated that the accuracy of identity recognition of MHPF-RS was improved, demonstrating the effectiveness and stability of the multi-haptic pressure feature.

Received Vovember29, 2013; revised .

doi:10.4304/jcp.9.9.2035-2042

2. HAPTIC PRESSURE COLLECTION

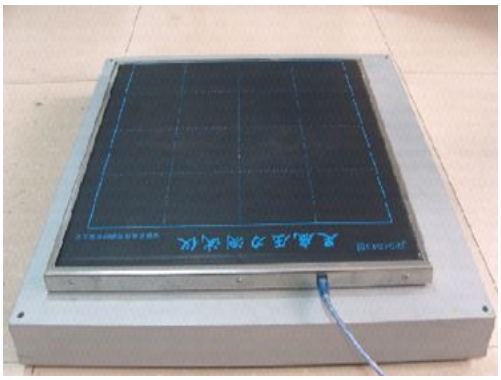

Figure 1. Photo-image showing one platform.

The platform system [6] for collection of haptic pressure was provided by the Key Laboratory of Biomimetic Sensing and Advanced Robot Technology of Intelligent Machines Institute of the Chinese Academy of Sciences. The platform system consists of 25 individual platforms, while each platform includes 2400 piezoresistive sensors with the size being 40 × 60 cm (Fig. 1). The measuring pressure range, sampling frequency, and measurement error of this platform are 10~900 kPa, 100 Hz, and 8%, respectively. Ten individuals (five males and five females, who are staff members or students in the Key Laboratory of Intelligent Computing & Signal Processing with the average age of 23.4 years) participated in this study. All of the individuals granted the permission to be tested, and they could move freely during the testing time. Sample data were collected under normal walking speed. Fig. 2 depicts the entire stage during one step: the heel landed first, the entire foot then landed with maximum pressure, and the toes landed at the end. As shown in Fig. 2, the pressure values could be represented by different colors; for example, red color marked with "a" represented pressure values in the range of 84-90 kPa.

3. FEATURE SET OF HAPTIC PRESSURE

3.1 Subset of Dynamic Feature

At present, these are many common dynamic haptic pressure features available, such as maximum pressure, total pressure value, average pressure, contact area, center of pressure, geometric center line, pressure change rate, and single contact time which are calculated according to table 1 [6, 7]. As mentioned in previous research, in order to solve the repeated problems of plantar pressure distribution in a normal population through the peak pressure, the maximum pressure point, the contact time, and the whole foot should be divided into ten regions [8]. On the other hand, in order to study the obesity influence of children and the adolescent in walking process through the dynamic plantar pressure distribution, the whole foot could be divided into five regions (i.e. big toe, 2-5toes, forefoot, arch, and heel) [9].

TABLE 1

CALCULATION FORMULA OF COMMON DYNAMIC FEATURE

Common Dynamic Feature	Calculation formula
Maximum pressure	$pre_{\max} = \max_{i=1\ldots n}\{pre_i\}$ i is an integer, i=1,2,…n
Total pressure	$\mathrm{pre}_{sum} = \sum_{i=1}^{n} \mathrm{pre}_i$
Contact area	$\mathrm{A}_{\mathrm{contact}} = \mathrm{a} * \sum_{i=1}^{n} \mathrm{i}$
Average pressure	$pre_{average} = \sum_{i=1}^{n} \mathrm{pre}_i / \mathrm{A}_{\mathrm{contact}}$
Center of pressure	$X_c = \sum_{i=1}^{n} (\mathrm{X}_i * \mathrm{pre}_i) / \sum_{i=1}^{n} \mathrm{pre}_i$ $Y_c = \sum_{i=1}^{n} (\mathrm{Y}_i * \mathrm{pre}_i) / \sum_{i=1}^{n} \mathrm{pre}_i$
Geometric center line	Geometric center line is the broken line which is formed by $\mathrm{pre}_{1c}, \mathrm{pre}_{2c}, \cdots \mathrm{pre}_{mc}$, being the center of every row.
Pressure change rate	$pre_R = \frac{d(pre_i)}{dt}$
Single contact time	$\mathrm{T}_{\mathrm{contact}}$ is the time from heel langding to toes leaving ground.

In this study, according to the related biometrics and the spatial resolution of equipment, the whole foot was divided into five regions (A1–A5) along the longitudinal axis of haptic pressure. The region of A1, A2, A3, A4, and A5 are heel, arch, forefoot, big toe, and 2-5 toes with relative contact area at 33%, 17%, 33%, 8.5%, and 8.5%, respectively. For each region, the dynamic feature subset was created by the regional feature, the ratio of length vs. width of external bounding rectangle, and the common dynamic haptic pressure feature. As shown in equation (1), the F_{h1}, F_{h2}, and F_{hs} are common dynamic features, regional features, and ratio of length to width, respectively. According to haptic pressure information, although pressure value was unstable, haptic pressure distribution was still relatively stable. So the regional feature of haptic pressure (mainly discussing the relation between regional pressure and whole pressure) was discussed in equation (2), where $F_{h2}(k)$ was the ratio of the k-th region pressure vs. total pressure, and pre_i was the pressure of each region, when it is greater than 2 kPa.

$$F_h = (F_{h1}, F_{h2}, F_{hs}) \tag{1}$$

$$F_{h2}(k) = \frac{\sum_{pre_i \in A_i} pre_i}{\sum_{k=1}^{5} \sum_{pre_i \in A_i} pre_i} \quad subject \quad to\, pre_i \geq 2KPa \quad k = 1, \cdots, 5 \tag{2}$$

The ratio of length vs. width feature was extracted since it is one of the most stable features in haptic pressure [10]. During walking, the axis cannot always keep horizontal or vertical, thus, the ratio of length vs. width of external bounding rectangle was extracted using the least area method[11].

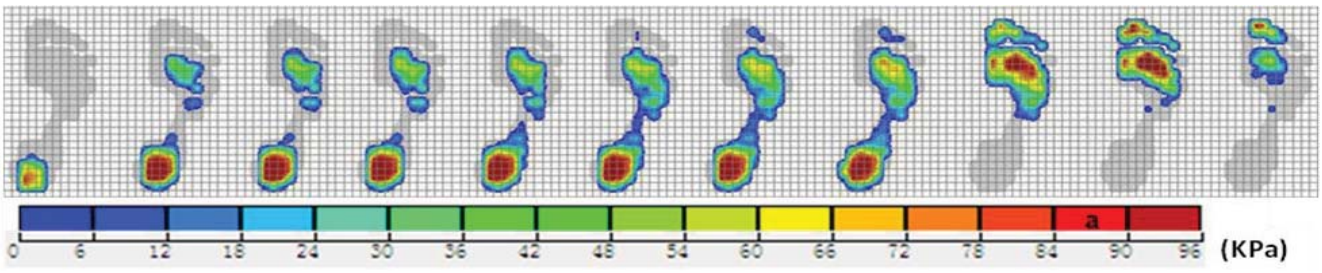

Figure 2. Entire stage of one step for haptic pressure

Below is the procedure to acquire the ratio of length vs. width:

(1) Selected centroid as the coordinate origin and main axis as the x axis.

(2) Rotated 5° per time (180° in total) to acquire the minimum area of bounding rectangle.

(3) Calculated the ratio of length vs. width of external bounding rectangle to obtain the F_{hs}.

3.2 Subset of Sparse Feature

Traditional approach for reconstructing images from measured data follows the well-known Shannon sampling theorem, in which the sampling rate must be at least twice as the highest frequency. The fundamental theorem of linear algebra also requires that the number of collected samples of discrete finite-dimensional signal should be at least as large as its length to ensure reconstruction. However, compressed sensing is a new type of sampling theory, which can predicts sparse signals and images reconstructed from incomplete information.

Based on the compressed sensing theory, if a vector I is K-sparse, it is possible to recover I from y. As shown in equation (3), $\Phi \in C^{m\ x\ N}$ is the measurement matrix, while the vector $y \in C^m$ is measurement vector. The main interest is vast under the sampled case of $m << N$.

$$y = \Phi I \tag{3}$$

According to statistics, many signals and images are not sparse in nature. However, at some suitable basis, its sparse representation could be obtained. In other words, the non-zero sparse could be acquired. Hence, the sparse representation of I can be obtained by equation (4). Where $I \in C^N$ is the normal signal of haptic pressure, $\Psi \in C^{N\ x\ N}$ is a sparse basis, and x is a sparse coefficient.

$$I = \Psi x \tag{4}$$

Then the whole measuring process is $y = \Phi\Psi x$, and signal can be recovered by equation (5).

$$\min \|s\|_1 \quad subject \quad to \quad \Phi\Psi s = y \tag{5}$$

Based on the sparse representation theory, the wavelet basis is a sparse basis. Thus, in this study, the sparse representation of haptic pressure is represented by wavelet basis.

The null space property (NSP) is difficult to express directly, while the restricted isometry property (RIP) is easier to handle and present[12]. If a matrix satisfies the conditions of RIP, then the sub-matrices (maximum column k) are the complete conditions. Gaussian, Bernoulli, and some deterministic matrices can satisfy the condition of RIP. Thus the Gauss, Bernoulli, and Topelitz matrices were usually chosen as the measurement matrices (shown in equation (6) and (7), respectively).

In theory, a random matrix (*e.g.*, the Gauss matrix and Bernoulli matrix) has the best random results. However, for the Gaussian/Bernoulli distribution, the free elements of Gauss/Bernoulli matrix (Φ(M×N) with $a_{i,j}$ ~N (0,1)) are both M×N, which is very high and should increase the data storage amount and cause the delay of real-time recognition. The deterministic matrix has been repeatedly reported in literatures [13-17]; the Topelitz matrix, as one of the deterministic matrices, has the free elements merely at N+M-1, which is much smaller than that of the Bernoulli matrix and Gauss matrix. Therefore, the Topelitz matrix was used for the measurement matrix in this study.

$$\varphi_{Guass \quad or \quad \text{Bernoulli}} = \begin{pmatrix} a_{11} & a_{12} \cdots & a_{1N} \\ a_{21} & a_{22} \cdots & a_{2N} \\ \vdots & \vdots & \vdots \\ a_{M1} & a_{M2} \cdots & a_{MN} \end{pmatrix} \tag{6}$$

$$\varphi_{topelitz} = \begin{pmatrix} a_N & a_{N-1} \cdots & a_1 \\ a_{N+1} & a_N \cdots & a_2 \\ \vdots & \vdots & \vdots \\ a_{N+M-1} & a_{N+M-2} \cdots & a_M \end{pmatrix} \tag{7}$$

In corresponding to various test measurement matrices, there are several algorithms to recover the signal, such as matching pursuit (MP)[18], orthogonal matching pursuit (OMP)[19], Improved Backward Optimized Orthogonal Matching Pursuit(MBOOMP)[20], regularized orthogonal matching pursuit(ROMP)[21], stagewise orthogonal matching pursuit(STOMP)[22], iterative hard thresholding (IHT)[23], compressive sampling matching pursuit (CoSaMP)[24] , subspace pursuit (SP)[25], *etc*. In this study, the SP was used to recover the signal since it has a good performance in reconstruction of probability and speed.

To facilitate the analysis, one-dimensional signal from haptic pressure was recovered based on the compressed sensing theory (the length of signal N was set as 256). The correlation between measurement times (or sparsity K) and the success rate of recovery were discussed in the following experiments.

TABLE 2

SUCCESS RATE *VERSUS* MEASUREMENT TIMES

Measurement matrix / Measure-ment times	Bernoulli matrix	Gaussian matrix	Topelitz matrix
50	1	0	0
55	2	2	1
60	5	6	8
65	20	19	27
70	43	40	51
75	82	77	80
80	87	90	93
85	97	99	98
90	99	100	100
95	100	100	100
100	100	100	100

TABLE 3

SUCCESS RATE *VERSUS* SPARSITY K

Measurement matrix / Sparsity K	Bernoulli matrix	Gaussian matrix	Topelitz matrix
20	100	100	100
25	100	100	100
30	84	86	90
35	42	37	38
40	8	7	8
45	0	0	0
50	0	0	0

The correlation of measurement times on the success rate of recovery was studied in the first experiment (sparsity K was set at 30). As shown in Table2 , the measurement times increased from 50 to 100 steps with a 5 steps interval, and the success rate of recovery based on the Bernoulli matrix, Gauss matrix, and Topelitz matrix improved with the increase of measurement times. Note that the success rate of Topelitz matrix was slightly higher than that of Bernoulli matrix and Gauss matrix, while the free element of Topelitz matrix was the least. In the second experiment (Table3), the measurement times (M) was set at 128, the success rate of recovery decreased when the sparsity K increased from 20 to 50. According to results from the above experiments, the Topelitz matrix was selected as the measurement matrix in the subsequent study, since it has the least free element and the highest success rate.

3.3 Dynamic Feature Optimization

Feature optimization is to choose some independent and reliable features from the numerous features, and it is an important step during the selecting parameters, which could directly affect the stability and unique of feature set.

The feature selection process consists of two steps, namely feature subset evaluation and feature subset search. Feature subset search process can be obtained through an optimal feature subset from the numerous feature subsets, which has the best evaluation function value of feature subset by using one of three search methods, such as exhaustive search, heuristic search and random search. From the point of view of the evaluation function, feature selection can be divided into five criterions, such as correlation measure, instance measure, information measure, consistency measure, and classification error rate [26]. In this study, by evaluating the feature subset evaluation function and saving all evaluated subsets, feature subset search was sequenced the feature subset in descending order according to its performance. And dynamic feature subset was optimized by correlation criterionAnd below is the procedure for feature optimization:

(1) Pre-treated the haptic pressure by denoising and removing the maximum pressure frame and two adjacent frames.

(2) Extracted the dynamic feature subset (F_h).

2a) Calculated the dynamic feature subsets (F_{h1} and F_{h2}) according to feature definition.

2b) Calculated the ratio of length vs. width of external bounding rectangle by using the least area method.

(3) Optimized the feature

(3.1) Calculated each feature (f_{hi}) and the $U(f_{hi}, F_h)$ according to the dynamic feature subsets (F_h), as shown in (8).

$$U(f_{hi},F_h)=2*\frac{En(f_{hi})+En(F_h)-En(f_{hi},F_h)}{En(f_{hi})+En(F_h)} \tag{8}$$

Where $En(f_{hi})=-p(f_{hi})\log_2 p(f_{hi})$ and

$En(F_h)=-\sum_{j=1}^{m} p(f_{hj})\log_2 p(f_{hj})$ are entropy function;

$En(f_{hi},F_h)=-\sum_{j=1}^{m} p(f_{hi},f_{hj})\log_2 p(f_{hi},f_{hj})$ is the joint entropy.

(3.2) Calculated the correlated evaluation function (H_s) of F_h according to equation (9).

$$H_s=\frac{\sum_i U(f_{hi},F_h)}{\sqrt{\sum_i\sum_j U(f_{hi},f_{hj})}} \tag{9}$$

(3.3) Obtained a new feature subset F_h' according to the descending order of $U(f_{hi}, F_h)$, dropped a feature with the smallest correlation, and calculated the evaluation function $H_s'^*$ again. If $H_s'^* \geq H_s$, the process should be repeated until no more decrease**.** The optimal subset $F_{ho}=(f_{h1}\cdots f_{hn})$ was created by the remained dynamic features.

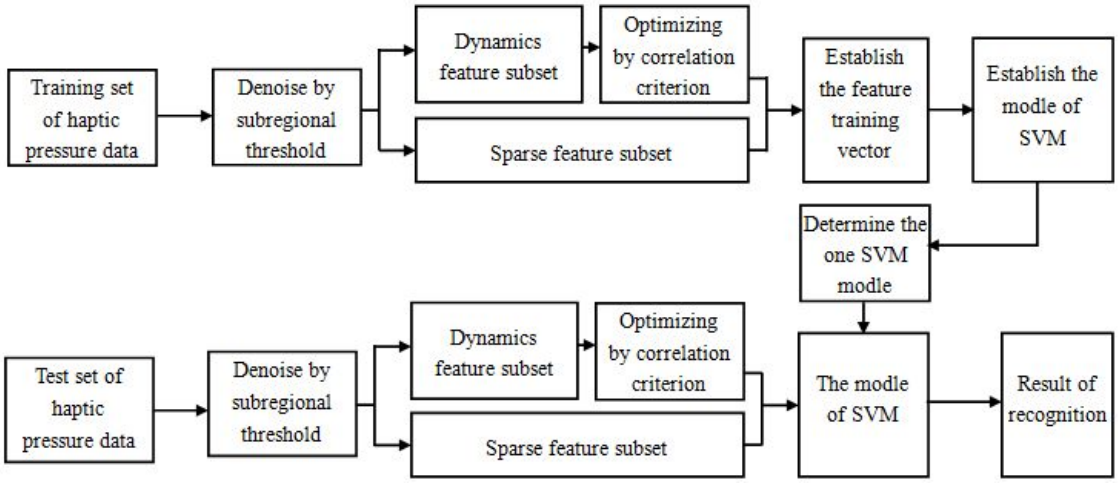

Figure 3. Block diagram of identity recognition

4. RESULT

For identity recognition, 90 samples per individual were collected among 15 steps, which included 45 left foot data and 45 right foot data. The data with the highest pressure value and two adjacent frame data were chosen, and the size of each frame was 32 × 64 pixel. The block diagram of identity recognition was shown in Fig. 3.

Firstly, samples of training set were denoised by sub-regional threshold. Then, common dynamic features, regional feature, and ratio of length vs. width of external bounding rectangle were extracted, which formed the dynamic feature subset. Meanwhile, the gray image of haptic pressure was obtained. Sparse representation of haptic pressure was acquired based on the wavelet basis, $I = \Psi x$, where Ψ is wavelet basis. The sparse feature vector F_r is obtained by using the Topelitz matrix as measurement matrix (i.e. $F_r = \Phi_{Topelitz} I$). The dynamic feature subset was optimized by correlation criterion, F_{oh} and F_r form feature set of haptic pressure, where F_{oh} was optimized feature subset. The classifier SVM followed the one to many rule to classify more than two objects. After that, the model of identity recognition based on MHPF-RS was obtained. Samples of test set were then input into the model, where F_r was extracted on the same measurement matrix. Thereafter, the SVM classifier output the identification result according to the rule of majority voting.

Different kernel functions have a certain effect on classification performance of SVM classifier. As we know, there are three commonly used kernel functions, Polynomial, Gaussian RBF, and Sigmoid. Polynomial kernel and Gauss RBF needs less input parameters. For the nonlinear classification, Gauss RBF is the best choice [27] and its application effect is very good in cancer classification and gait recognition [28, 29].

Meanwhile penalty factor C and kernel function parameter γ selection also have a certain influence on classification performance of SVM classifier. The penalty factor C not only controls punishment degree of misclassified samples, but also determines complexity and generalization ability of model. The kernel function parameter γ determines the mapping feature space (dimension), thus affecting the minimum empirical error of classification. According to the experiment result, Gaussian RBF has been eventually selected in this study, and at the same time penalty factor C and kernel function parameter γ are 10, 4 respectively.

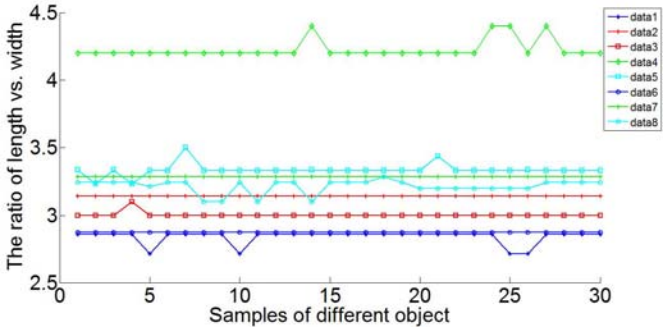

Figure 4. The curve of dynamic feature

The dynamic feature (i.e. ratio of length vs. width) was studied in the first experiment. During the study, eight curves for each individual object were acquired according to the haptic pressure, and each curve contained 30 data at different sampling time (each data is the average of 20 frames); meanwhile, the ratio of length vs. width of external bounding rectangle were acquired by the least area method. As shown in Fig. 4; the average feature value fluctuated up and down within the range of 4.36%, while eight curves are easy to distinguish.

For the second experiment, the regional features of forefoot and heel were studied and shown in Fig.5a and 5b, respectively. The results indicated that the regional features fluctuated barely, while eight curves are easy to identify.

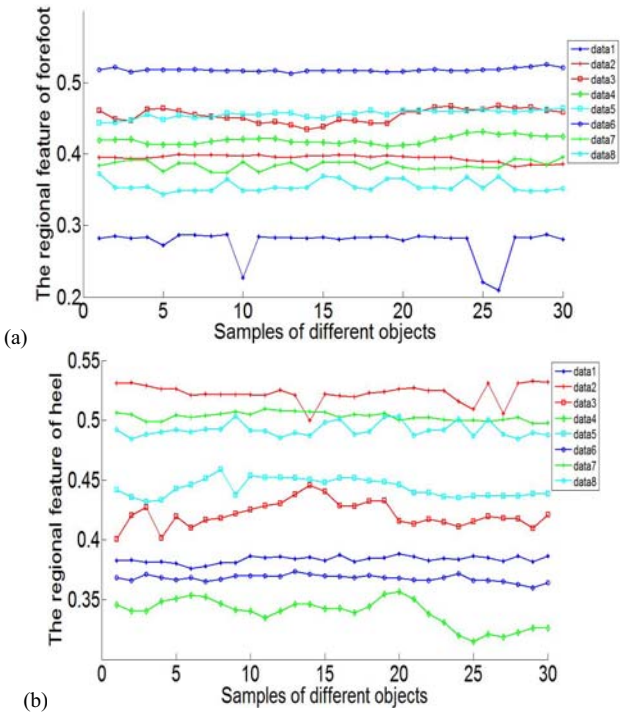

Figure 5. (a) The curve of the regional feature of forefoot. (b) The curve of the regional feature of heel

In order to further discuss the stability and repeatability of features, intraclass correlation coefficient (ICC) and coefficient of variation (C.V) were calculated. ICC, as shown in equation (10), is one of the index to evaluate the reliability and repeatability of object [30]. According to the ICC standard, [0, 0.4] shows poor reliability and [0.75, 1] shows the good reliability [31]. The ICC of 8 objects were summarized in table4, where F_{hs} is the ratio of length vs. width, and $f_{h2}(1) - f_{h2}(5)$ are regional features of region 1–5. It shows in table4 that, the confidence of F_{hs} has the best average value at 0.9798, while, the $f_{h2}(1)$ and $f_{h2}(3)$ also maintained good confidence, however, a few confidences of $f_{h2}(2)$, $f_{h2}(4)$, and $f_{h2}(5)$ are quite low.

$$ICC = \frac{2\sum_{i=1}^{n}(x_{i1}-\bar{x})(x_{i2}-\bar{x})}{\sum_{i=1}^{n}(x_{i1}-\bar{x})^2+\sum_{i=1}^{n}(x_{i2}-\bar{x})^2},\ \bar{x} \text{ is average} \quad (10)$$

$$C.V = \frac{\text{standard deviation}}{\text{average}} * 100\% \quad (11)$$

Furthermore, as demonstrated in equation (11), C.V could be used to measure the variation degree of sample, which eliminates the influence of sample units and the average value. As shown in table5, the result of C.V is consistent with that of ICC, in which the C.V of $f_{h2}(2)$, $f_{h2}(4)$, and $f_{h2}(5)$ are high, and the highest C.V happening in $f_{h2}(5)$ reached up to 116.83%, while the C.V of other feature is lower than 10%. Note that $f_{h2}(2)$, $f_{h2}(4)$, and $f_{h2}(5)$ are the features of big toe, 2-5toes, and arch, respectively. In these three regions, haptic pressure and contact area are small and easily affected by environmental and standing posture, thus, the coefficient of variation is high for different measures. And ref [10] has been also described that the heel and the forefoot regions are the highest stability, which bear most of haptic pressure value.

TABLE 4

THE INTRACLASS CORRELATION COEFFICIENT OF 8 OBJECTS

Number	$f_{h2}(1)$	$f_{h2}(2)$	$f_{h2}(3)$	$f_{h2}(4)$	$f_{h2}(5)$	F_{hs}
1	0.9996	0.9722	0.9964	0.9201	0.9987	1.0000
2	0.9730	0.9976	0.9870	0.9569	0.9913	0.9702
3	1.0000	0.9328	0.9918	0.9893	0.9957	1.0000
4	0.9499	0.9064	0.9506	0.5940	0.9983	0.8980
5	0.9308	0.9997	0.9997	0.9999	0.9998	1.0000
6	0.9648	0.9998	0.8958	0.8101	0.8185	1.0000
7	0.8777	0.6725	0.7645	0.7740	0.7112	0.9702
8	0.9517	0.9998	0.9433	0.9728	0.9855	1.0000

TABLE 5

COEFFICIENT OF VARIATION OF 8 OBJECTS

C.V（%）

Number	$f_{h2}(1)$	$f_{h2}(2)$	$f_{h2}(3)$	$f_{h2}(4)$	$f_{h2}(5)$	F_{hs}
1	1.57	3.88	1.22	5.40	96.23	7.4205E-16
2	0.68	14.65	1.59	9.04	38.26	2.92
3	3.03	2.72	3.51	6.00	116.83	4.56
4	2.20	27.82	1.19	4.04	4.21	1.58
5	0.72	5.34	9.33	25.98	24.88	1.81
6	1.25	1.29	1.46	3.65	6.04	0
7	6.10	3.93	4.09	14.13	8.40	1.74
8	0.78	2.22	0.50	1.48	2.35	4.8697E-16

For the third experiment, four algorithms by using different feature set were compared, which included common dynamic feature, multi-dynamic feature, multi-dynamic feature after correction, and multi-haptic pressure feature based on sparse representation. For all algorithms, the SVM classifier followed the one to many rule. Among 450 samples of left foot (45 samples × 10 objects), 60% samples for each object were randomly selected as training samples to establish the model of identity recognition, while the rest samples were used as test samples. Accuracy is average of 50 tests repeating 3 times. Table6 shows the results of accuracy based on four different algorithms, it is evident that the algorithm using MHPF-SR has the average accuracy up to 96.81% among those 4 algorithms.

TABLE 6

THE ACCURACY OF ALGORITHMS USING DIFFERENT FEATURE SETS

Feature set	Accuracy (%)			Number of error		
Common dynamic feature	71.11	72.00	64.44	52	50	64
Multi dynamic feature	67.56	63.56	71.11	58	66	52
Multi dynamic feature after correction	86.67	87.11	88.89	24	23	20
Multi haptic pressure feature	95.56	98.43	96.44	8	3	6

5. CONCLUSION

In this study, a new identity recognition method of multi-haptic pressure feature based on sparse representation was investigated according to the common dynamic features such as regional feature and the ratio of length vs. width of external bounding rectangle (extracted by using the least area method). The subset of dynamic feature was optimized by correlation criterion, the sparse representation of haptic pressure was obtained according to the sparse basis, and the sparse feature vector was calculated by the Topelitz measurement matrix. Then, the haptic pressure feature set was obtained by combining optimized dynamic feature subset and sparse feature subset. Furthermore, SVM classifier was used and the identification result was yielded according to the rule of majority voting. The results of ICC and C.V evidenced the stability of features, while the highest accuracy of identity recognition based on MHPF-RS exceeded 98.43%, demonstrating effectiveness and stability of the algorithm. The future research will investigate feature set which will be obtained by using different combining method.

ACKNOWLEDGEMENTS

We will appreciate valuable comments on an earlier version of this paper from the anonymous referees.We also express our thanks to Professor Yi-ning Sun for valuable guidance and helpful discussions. Helpful discussions with Professor Fong is also acknowledged. This work was partly supported by the National Natural Science Foundation of China(Grants No.: 61172127 and 61201127); the Doctoral Program of Higher Education (Project No.: 20113401110006), and the Youth Research Project of Anhui University (Project No.: KJQN1107).

REFERENCES

[1] D..Surdilovic, Z. Jinyu. Gait phase and centre of pressure measuring system [J]. Industrial Informatics, 2004 2nd IEEE International Conference, INDIN, 2004, 331-334.

[2] P.R.Cavanagh, J.S.Ulbrecht, G.M Caputo. New developments in the biomechanics of the diabetic foot. Diab Metab Res Rev 2000;16:S6–10.

[3] D. L. Edward, B. Ajoy. Plantar pressure parameters for dynamic gait stability analysis [J]. Engineering in Medicine and Biology Society. EMBS '06. 28th Annual International Conference of the IEEE, 2006, 4465-4468.

[4] A. B. Putti, G. P. Arnold, L. A. Cochrane, R. J. Abboud. Normal pressure values and repeatability of the Emed ST4 system[J]. Gait Posture, 2008, 27(3), 501-505.

[5] A. Ramanathan, G. Fadel, A. Jain, R. Abboud. Press-fit ceramic implant arthroplasty of the Hallux Metatarsophalangeal joint-evaluation of outcomes[J]. Foot, 2008, 18, 34-39.

[6] S. Xu, X. Zhou, Y. Sun. A genetic algorithm-based feature selection method for human identification based on ground reaction force[J]. Proc of the 1st ACM/SIGEVO Summit on Genetic and Evolutionary Computation, Shanghai, China, 2009, 665-670.

[7] Z.M.Yao. Gait recognition based on haptic force information[D]. Hefei, University of Science & Technology of China, 2010, 91-98 (in Chinese).

[8] J. K. Gurney, U. G. Kersting, D. Rosenbaum. Between-day reliability of repeated plantar pressure distribution measurements in a normal population[J]. Gait Posture, 2008, 27, 706-709.

[9] S. H. Hua, Yan, K. Zhang, G. Q. Tan, J. Yang, Z. C. Liu. Effects of obesity on dynamic plantar pressure distribution in Chinese prepubescent children during walking [J]. Gait & Posture, 2013, 37(1), 37-42.

[10] B. Kerstin, G. Joachim. Preliminary normative values for foot loading parameters of the developing child [J]. Gait & Posture, 2007, 26(2), 238-247.

[11] C.G. Rafael, E.W. Richard. Digital image processing, Third Edition[M]. Beijing, Publishing house of electromcs industry, 2010, 801-861.

[12] E.J. Candès and T. Tao. Decoding by linear programming[J]. IEEE Trans. Inform. Theory 51 (2005), 4203–4215.

[13] W. U. Bajwa, J. D. Haupt, G. M. Raz, S. J. Wright, R. D. Nowak. Toeplitz-structured compressed sensing matrices[J]. Proceedings of the 2007 IEEE/SP 14th Workshop on Statistical Signal Processing, 2007, 294-298.

[14] H. Rauhut. Circulant and Toeplitz matrices in compressed sensing[R]. Proc. SPARS'09, 2009, http://arxiv.org/abs/0902.4394.

[15] R. Devore. Deterministic constructions of compressed sensing matrices[J]. Journal of Complexity, 2007, 23, 918-925.

[16] J. Haupt, W. U. Bajwa, G. Raz, R. Nowak. Toeplitz compressed sensing matrices with application to sparse channel estimation[J]. IEEE Transactions on Information Theory, 2010, 56(11), 5862-5875.

[17] K. Wang, Y. Liu, J. Zhang. RIP analysis for quasi-Toeplitz CS matrices[J]. 2010 International Conference on Future Information Technology and Management Engineering (FITME), 2010, 2, 9-10.

[18] S. Mallat and Z. Zhang. Matching pursuit in a time-frequency dictionary[J]. IEEE Trans Singal Processing, 1993, 41(12), 3397–3415.

[19] J . Tropp , A. Gilbert . Signal recovery from ran dom measurement s via ort hogonal matching pursuit [J] . IEEE Trans. Inform. Theory , 2007, 53 (12) , 4655–4666

[20] F.Hong, Z.Quanbing, W.Sui. Image Reconstruction Based on Improved Backward Optimized Orthogonal Matching Pursuit Algorithm[J]. Journal of South China University of Technology, 2008,36（8）,23–27(in Chinese).

[21] D. Needell , Vershynin R. Uniform uncertainty principle and signal recovery via regularized orthogonal matching pursuit [J] . Found. Comput . Math, 2009 ,9 (3) : 317–334.

[22] D. L. Donoho, I. Drori, Y. Tsaig, and J. L. Starck. Sparse solution of underdetermined linear equations by stagewise orthogonal matching pursuit[R]. Technical Report, Stanford Univer sity, 2006.

[23] T.Blumensath and M.Davies. Iterative hard thresholding for compressed sensing[J]. Appl. Comput. Harmon. Anal., 2009, 27(3): 265–274.

[24] D. Needell and J. A. Tropp. CoSaMP: Iterative signal recovery from incomplete and inaccurate samples[J]. Appl.AndComp.Harm.Anal, 2009, 26(3):301–321.

[25] W. Dai and O. Milenkovic. Subspace pursuit for compressive sensing signal reconstruction [J]. IEEE Trans. Inform. Theory, 2009, 55(5): 2230–2249.

[26] M .Dash, Liu H. Feature selection for classification[J]. Intelligent Data Analysis, 1997.1(3):131-156.

[27] C.Burges A tutorial on support vector machines for pattern recognition[J]. Data Mining and Knowledge Discovery, 1998, 2(2): 121-167.

[28] S. Moustakidis, Theocharis J, Giakas G. Subject Recognition Based on Ground Reaction Force Measurements of Gait Signals[J]. IEEE transactions on systems, man, and cybernetics Part B, Cybernetics: a publication of the IEEE Systems, Man, and Cybernetics Society, 1998. 38(6):1476.

[29] S.Wang, J.Wang, H .Chen, S .Li. Feature extraction and classification of tumor based on wavelet package and support vector machines[J]. Advances in Knowledge Discovery and Data Mining, 2007.871-878.

[30] J .Bartko. The intraclass correlation coefficient as a measure of reliability [J]. Psychological reports, 1966, 19(1), 3-11.

[31] B. Bilney, M. Morris, K .Webster. Concurrent related validity of the GAITRite(R) walkway, system for quantification of the spatial and temporal parameters of gait [J]. Gait & Posture, 2003, 17(1), 68-74.

YanZhang was born in 1982 from XuanChen, received M.SC. in 2003. Now she is Ph.D candidate in Anhui University. Her research field includes image processing, pattern recognition, etc. E-mail: zhangyaner2005@163.com.

DongLiang was born in 1963 from HeFei, received M.SC. in 1990 and Ph.D. in 2002, from Anhui University China. Now he is a professor and doctoral supervisior in Anhui University. His research field includes image processing, computer signal processing, pattern recognition, etc. E-mail: dliang@ahu.edu.cn. Telephone:+86- 0551-63861275.